Feasibility of coded vibration in a vibro-ultrasound system for tissue elasticity measurement

Jinxin Zhao, Yuanyuan Wang, Jinhua Yu, et al.

Citation: The Journal of the Acoustical Society of America **140**, 35 (2016); doi: 10.1121/1.4954738
View online: https://doi.org/10.1121/1.4954738
View Table of Contents: https://asa.scitation.org/toc/jas/140/1
Published by the Acoustical Society of America

Feasibility of coded vibration in a vibro-ultrasound system for tissue elasticity measurement

Jinxin Zhao, Yuanyuan Wang,[a),b)] and Jinhua Yu[b)]
Department of Electronic Engineering, Fudan University, Shanghai 200433, China

Tianjie Li and Yong-Ping Zheng
Interdisciplinary Division of Biomedical Engineering, The Hong Kong Polytechnic University, Hong Kong Special Administrative Region, China

(Received 20 October 2015; revised 8 June 2016; accepted 11 June 2016; published online 5 July 2016)

The ability of various methods for elasticity measurement and imaging is hampered by the vibration amplitude on biological tissues. Based on the inference that coded excitation will improve the performance of the cross-correlation function of the tissue displacement waves, the idea of exerting encoded external vibration on tested samples for measuring its elasticity is proposed. It was implemented by integrating a programmable vibration generation function into a customized vibro-ultrasound system to generate Barker coded vibration for elasticity measurement. Experiments were conducted on silicone phantoms and porcine muscles. The results showed that coded excitation of the vibration enhanced the accuracy and robustness of the elasticity measurement especially in low signal-to-noise ratio scenarios. In the phantom study, the measured shear modulus values with coded vibration had an $R^2 = 0.993$ linear correlation to that of referenced indentation, while for single-cycle pulse the R^2 decreased to 0.987. In porcine muscle study, the coded vibration also obtained a shear modulus value which is more accurate than the single-cycle pulse by 0.16 kPa and 0.33 kPa at two different depths. These results demonstrated the feasibility and potentiality of the coded vibration for enhancing the quality of elasticity measurement and imaging.
 [http://dx.doi.org/10.1121/1.4954738]

[GH] Pages: 35–44

I. INTRODUCTION

Tissue elasticity assessment plays an important role in medical diagnosis. Elastography techniques, which measure or image the tissue elasticity using ultrasound or magnetic resonance imaging, have experienced a rapid development and made great achievements in the past two decades.[1–13] The history of elastography can be dated back to the early 1990s. Several groups[1,2,14,15] proposed different methods for the visualization of the elasticity within biological tissues. Afterward, Fink *et al.* proposed the concept of transient elastography (TE).[4,5,16,17] The high imaging frame rate of TE makes it insensitive to patient movements, while sonoelastography[18] requires a relatively static tissue due to its long data acquisition time. Besides these methods using imposed mechanical vibration at tissue surfaces, the scheme of generating internal vibration by an amplitude-modulated beam of focused ultrasound was also proposed.[3,4,19] The internal displacement can be used to measure either local elasticity, as in acoustic radiation force imaging (ARFI),[19,20] or remote elasticity property by detecting the shear waves as in shear wave elasticity imaging (SWEI).[3,21] Later, the supersonic shear imaging (SSI) was proposed[7] to provide quantitative shear modulus mapping of tissues with a high frame rate, which ensures a real-time visualization of the two-dimensional (2-D) elasticity map. Since biological tissues are usually dispersive to shear waves, shear wave dispersion ultrasound vibrometry (SDUV) method was developed to measure both elasticity and viscosity.[8,22] Its validation was demonstrated in the measurement of kidney[23] and liver fibrosis.[24]

In all elastography methods, the detection of tissue displacement waves plays an important role with either internal or external vibration source. The displacement wave is detected by estimating the temporal shift of ultrasound radio-frequency (RF) lines between two consecutive frames. The most commonly used method is the cross-correlation technique.[1,2,25,26] After estimating the displacements, the elasticity could be computed based on the estimated velocity of the tissue movements, which is calculated from the propagation distance and the time difference of displacements.[8,9,27] To pursue an accurate elasticity measurement, a displacement wave with a high signal-to-noise ratio (SNR) is desired. This accords with the fact that a larger shear wave amplitude and a higher pulse-echo SNR (leading to less noise in the displacement estimation) are helpful to minimize the error of the measurement.[28] One of the most effective ways to improve the SNR of detected waves is to increase the excitation amplitude in pulse excitation.[29] However, in clinical application, a lower excitation amplitude and a further detectable distance are preferred if the measurement accuracy can be achieved.[23,30–32] These will lead to the decrease of the detected displacement wave amplitude and thus the SNR of the displacement wave. With the same excitation amplitude, we proposed to apply coded excitation of the vibration in tissue elasticity measurement.

[a)]Electronic mail: yywang@fudan.edu.cn
[b)]Also at: Key Laboratory of Medical Imaging Computing and Computer Assisted Intervention (MICCAI) of Shanghai, Shanghai 200433, China.

Coded excitation has been demonstrated to be an effective approach for improving penetration without the loss of resolution in ultrasound imaging and diagnosis.[29,33–40] It utilizes the pulse compression technique to extend the bound of the tradeoff between the resolution and penetration in ultrasound imaging.[36] The optimal detection SNR was obtained by decoding the transmitted wave using a matched filter to compress the energy into a short time interval. Compared with single-cycle pulse, the energy of a coded wave was enhanced by longer pulse duration, with coding technique to compress the decoded wave duration. In a recent study,[41] the enhancement of shear wave motion detection by the coded ultrasound imaging has also been demonstrated. The increase of pulse-echo SNR by the coded excitation of the ultrasound signal promised higher robustness of the elasticity measurement.

Unlike the coded ultrasound imaging, we adopted coded excitation for mechanical vibrations instead of the longitudinal ultrasound pulses[41] for the elasticity measurement. In coded ultrasound imaging for elastography, the ultrasound penetration and SNR is improved to benefit the elasticity measurement. For our proposed method, it is desired that the coded vibration would enhance the detection of shear waves with small amplitudes. The idea was validated by a vibro-ultrasound elasticity measurement system, which has been developed in previous studies.[27] The system used an external vibration source, and measured the elasticity by tracking the shear wave. Unlike previous studies, which used a ten-cycle wave excitation and a complicated pair peak value detection algorithm,[27] we took advantage of the low sidelobe characteristic of coding technique. The time shift between different displacements was estimated by simply detecting the peak value time in the cross-correlation function (CCF). This estimation was also conducted using a single-cycle vibration pulse as a comparison. Experiments were conducted on both silicone phantoms and porcine muscle tissues, which is a typical material in elasticity studies.[42,43] The results showed that compared with traditional pulse excitation, coded excitation of the vibration enhanced the robustness of the elasticity measurement against noise and increased the measurement accuracy in low SNR scenarios. This is potential for improving measuring distance and sensitivity of elastography.

The rest of the paper is organized as follows. The background of coded excitation is presented in Sec. II. Section III describes the system platform together with the materials and methods used in the experiments. Then in Sec. IV the results are given. Section V presents a discussion of the result. Finally, a conclusion is drawn in Sec. VI.

II. BACKGROUND OF CODED EXCITATION

Coded excitation is an approach that uses the pulse compression technique to improve SNR[29,33] or to extract material nonlinearity.[12] Compared with the uncoded pulse of the same length, the effect of coding is to decrease the range sidelobe level (RSLL), which is the ratio between the mainlobe peak value and the sidelobe peak value of the matched filter output (autocorrelation of the pulse).[36]

The most commonly used codes are the linear chirp code, Barker code, and Golay pair code.[36] Chirp code is a frequency-modulated code. It has a time-dependent instantaneous frequency and could be expressed as[36,38]

$$S(t) = w_0(t)e^{j(2\pi f_0 t+\alpha t^2/2)}, \tag{1}$$

where f_0 is the center frequency, $w_0(t)$ is the apodization window for the envelope, and α represents the frequency changing rate. The chirp code has been used widely in ultrasound imaging and demonstrated to have high energy concentration with a proper filter.[36,38] Barker code and Golay pair code are both phase modulated codes. Currently, a few Barker code sequences have been proposed. A widely used one is a kind of pseudorandom binary sequence, whose autocorrelation function $R(m)$ satisfies

$$R(m) = \sum_{k=1}^{N-|m|+1} c_k c_{k+m} = \begin{cases} N, & \text{for } m = 0 \\ 0, & \text{for } m \neq 0, \end{cases} \tag{2}$$

where c_k is the code sequence, N is the sequence length, m is the time step difference and should have an absolute value less than N. For the ideal compression of RSLL, the Barker code is also seen as the optimum binary code.[36] The third kind, Golay pair code, requires two transmissions. Its pair complementarity characteristic is able to perfectly cancel the RSLL

$$\sum_{k=1}^{N-|m|+1} a_k a_{k+m} + \sum_{k=1}^{N-|m|+1} b_k b_{k+m} = \begin{cases} 2N, & \text{for } m = 0 \\ 0, & \text{for } m \neq 0, \end{cases} \tag{3}$$

where a_k and b_k are two complementary code sequences. This is known as the complementarity condition,[36] which requires the transmissions of the pair codes with the same parameters.

Not all these codes are suitable for the application in elasticity measurement. Biological tissues are commonly dispersive.[44] Thus, the chirp code, which usually has a relatively wide bandwidth to achieve good pulse compression performance, required careful design to be applied in the elastography study. The potential dispersion deformation of the shear wave through its propagation may destroy the linear modulation characteristic and thus introduce error into the post matched filtering. The Golay pair code is also not a good option. Besides the longer measuring time, as it requires two times of excitation, its complementarity condition is also sensitive to potential tissue movements.

In contrast, Barker code (4-bit in this paper) may be relatively easier to be applied in elasticity measurement. In coded ultrasound imaging, the RF data are first decoded and then beamformed after acquisition.[33,36,38] With white noise assumption, the optimum output is the autocorrelation of the coded waveform and is obtained by designing a matched filter.[36] Since the energy of several digit pulses is concentrated, the SNR is increased compared with the single-cycle pulse. Meanwhile, the RSLL in the output maintains relatively comparable as that of the single-cycle pulse, which benefits

the detection of the peak value. Due to the fact that the matched filter output is the autocorrelation,[36] the CCF of two waveforms at different positions should also have an increased SNR and low RSLL, with the assumption that there is only time shift without any significant deformation between the two waveforms.

On the other hand, the high RSLL in the CCF of an uncoded multi-cycle pulse[33,36] may make CCF peak value time hard to distinguish. Figure 1 gives a comparison between the 4-bit uncoded wave and the Barker coded wave. A central frequency of 100 Hz was set and the Barker code has a pulse sequence of [1,1,1,−1].[36] The time shift of two waves [Figs. 1(a) and1(b)] was set to be 5 ms, which corresponds to the moment when the peak value of the CCF comes in Fig. 1(d). Although in Fig. 1(c) the peak value also arrives at the same time, we can see the higher first sidelobe makes the mainlobe peak value not as remarkable as in Fig. 1(d). The peak value time will be harder to distinguish and more sensitive to noise if a larger cycle number is used, which will narrow the difference between the mainlobe peak and the first sidelobe peak.

As used to increase the penetration while maintaining the resolution in ultrasound imaging, we utilized the low RSLL in the CCF of the coded pulse to enhance the estimation of wave time shift by using the CCF peak value time. By comparison with a single-cycle pulse which also has a low RSLL, the Barker coded wave should benefit the accuracy and robustness of the estimation as it had higher concentrated energy. An example is given in Fig. 2.

In Fig. 2, both the single pulse and the 4-bit Barker pulse are contaminated with a −6 dB (half-amplitude) zero-mean, Gaussian-distributed noise. The noise will introduce interference to the CCF, which can lead to the inaccuracy of the peak value time. The CCF of the coded wave, by comparison, showed fewer burrs in the mainlobe, resulting from the higher energy. The peak value time is also closer to the real value 5 ms. This shows the higher robustness brought by the coding technique.

III. METHODS AND MATERIALS

This section will give a description of the vibro-ultrasound system, the data processing procedure, the materials, and the experiment designs.

A. Vibro-ultrasound system with coding module for elasticity measurement

A vibro-ultrasound system for muscle elasticity measurement was presented in a previous study.[27] The system was aimed at characterizing the skeletal muscle stiffness in the muscle action direction and was successfully applied in measuring the vastus intermedius (VI) stiffness (shear modulus). In the system, a mechanical vibrator was used to generate a ten-cycle pulse. Time shifts were averaged between each pair of the wave peaks to increase the accuracy, which required a complex peak value detection algorithm. In this study, we proposed to use Barker coded vibration in the elasticity measurement system. Due to the low RSLL, time shifts could be estimated by just detecting the CCF peak value time. We realized the proposed idea by integrating the vibro-ultrasound system with a vibration control module. Experiments were conducted on both silicone phantoms and porcine muscles to evaluate the coded vibration concept. Figure 3 gives the diagram and a photo of the measurement system.

An electromagnetic vibrator (4810, Brüel & Kjær, Nærum, Denmark), which was driven by a power amplifier and controlled by an arbitrary function generator (AFG3021, Tektronix, Beaverton, OR), was used to induce shear waves. Both coded and uncoded vibrations were generated for the measurement, and the electrical signal was then amplified to 0.5 V/0.1 A to drive the electromagnetic vibrator. To reduce the anisotropic effects, a short straight push bar was mounted

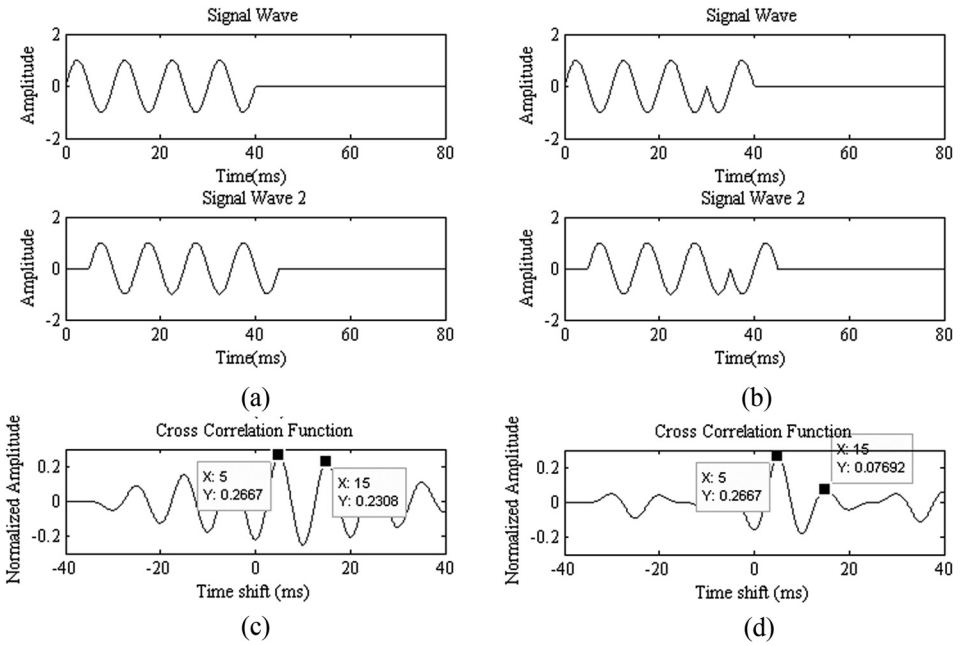

FIG. 1. A comparison between the 4-bit uncoded wave and the Barker coded wave for time shift estimation using the CCF: (a) and (b) are two 4-bit Barker codes of the same pulse sequence with a 5-ms time shift, (c) is their CCF, in which the peak value time corresponds with the 5-ms time shift.

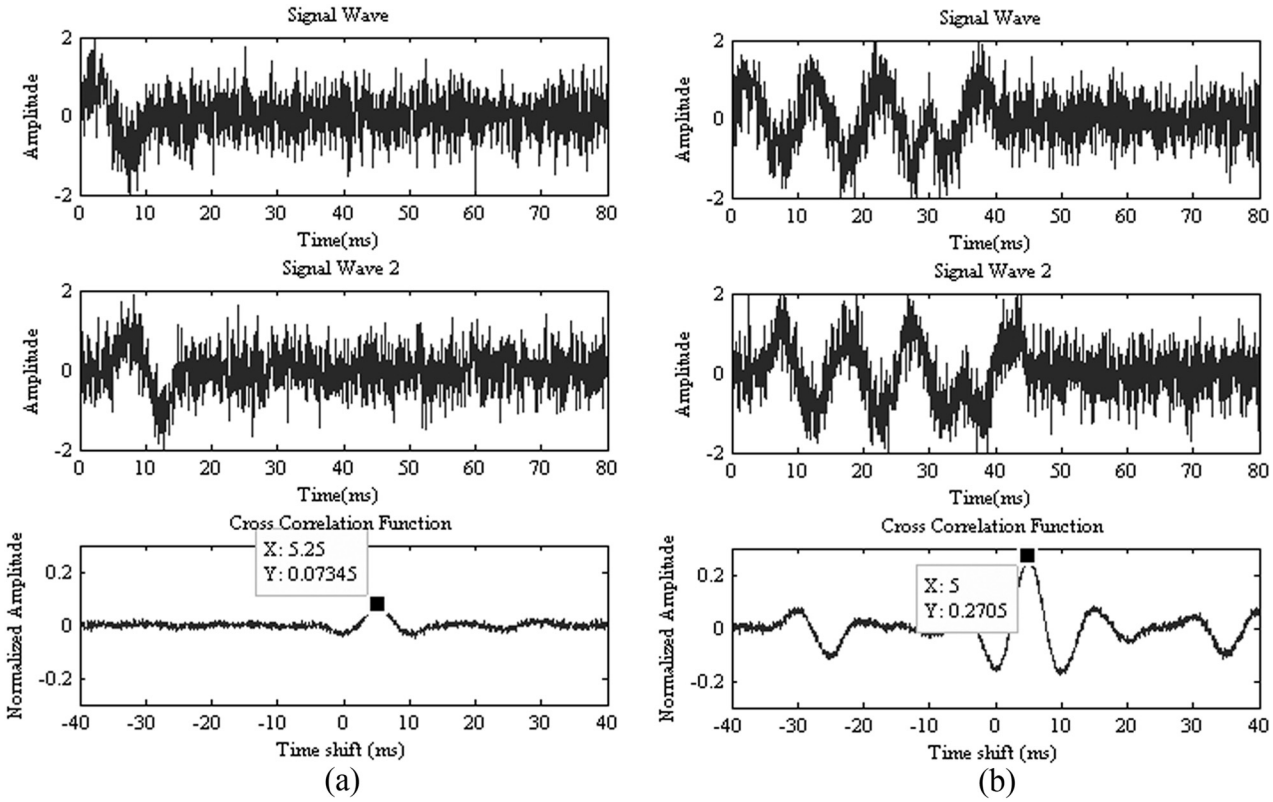

FIG. 2. Comparison between (a) the single sinusoidal pulse and (b) the 4-bit Barker codes under the −6 dB noise scenario.

to induce the vibration and its direction was adjusted perpendicular to the surface of the material. The vibration then generated horizontally propagated shear waves.[27] For the vibration frequency, to avoid rapid attenuation, 100 Hz wave was used for the silicone phantom and this value comes down to 25 Hz for the porcine muscle. And since shear wave velocities may be small in soft tissues, a long pulse may be overlapped with the probable boundary reflected wave. The 4-bit length of the coded wave was selected to avoid too long pulse duration.

For the detection of the shear wave, two predefined scan lines with a distance of 15.4 mm were tracked using a commercial ultrasound scanner SonixRP (Ultrasonix Medical Corp., Vancouver, Canada) with a 9.5-MHz transducer (L14–5/38, Ultrasonix). The M-mode data of the two scan lines were then used for detecting the shear waves. The frame rate was 4.7 kHz, which ensures sufficient sampling of the shear wave according to the Shannon-Nyquist sampling theory.

B. Data processing procedure

All data processing procedures were conducted off-line using the software MATLAB (R2013a, MathWorks, Inc., Natick, MA). The data processing algorithm includes the following main steps: (1) to acquire the displacement waveforms at a predefined depth from the temporal RF data; (2) to estimate the time shift between the displacement waveforms of two scan lines and calculate the shear wave velocity; (3) to compute the corresponding elasticity of the tissue.

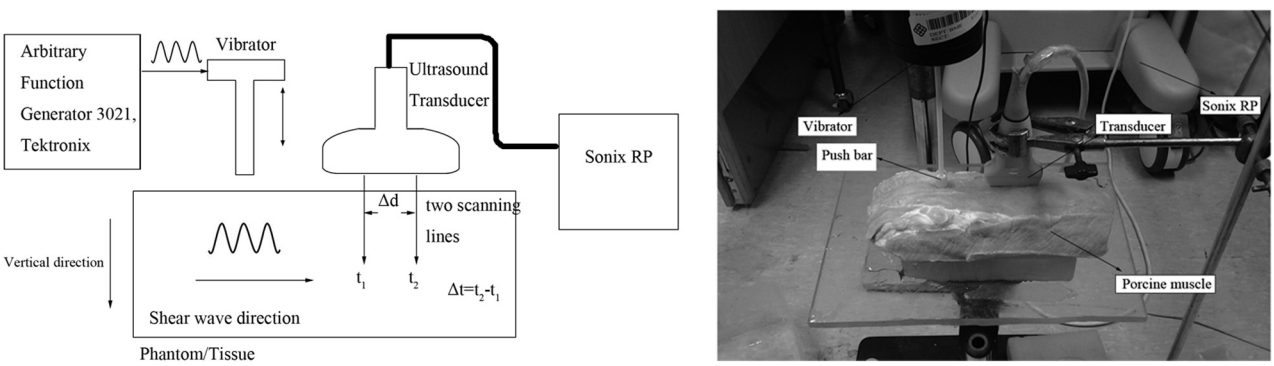

FIG. 3. (a) The diagram of the vibro-ultrasound system for elasticity measurement; (b) a photo of the measuring system.

For the conversion from the temporal RF signals to the tissue displacement wave, the normalized cross-correlation algorithm is a classical echo-tracking method.[2,4,5,20,27] It is based on the estimation of the time shift between two consecutive frames of RF lines by computing the cross correlation of two divided segments with the same length. This length was set 1 mm in this study. The estimated time shifts are then used to compute the shear wave amplitude with the knowledge of the ultrasound RF sampling rate (40 MHz) and the speed of ultrasound (generally, 1540 m/s in soft tissues). After the acquisition of the displacement waveforms, an interpolation factor of 10 was used to improve the temporal resolution before the CCF of them is computed. Based on the assumption that no significant deformation between the two waves exists, the peak value time corresponds to their time shift Δt. Then the shear velocity c_s, typically on the order of 1 m/s in biological tissues,[25] could be estimated by

$$c_s = \Delta d/\Delta t, \tag{4}$$

where Δd is the distance between the scan lines as shown in Fig. 3(a). The shear wave velocity is related to the shear modulus μ. In a simple model,[27] their relationship could be expressed as

$$\mu = \rho c_s^2, \tag{5}$$

where ρ represents the mass density and c_s is the shear wave velocity.

C. Materials

Tissue mimicking silicone phantoms were made by mixing the silicone rubbers (E650, Shenzhen Hongyejie Technology Co. Ltd, Shenzhen, China) and the silicone oil AK-35 (Wacker Chemicals Hong Kong Ltd., Hong Kong, China). The ratios between the silicone and the oil were 1:4, 1:3, 1:2, 1:1.5, 1:1, 1:0.5, and 1:0, corresponding to an increasing stiffness (numbered as phantoms 1–7). Curing agents of the same weight as the silicone rubbers were also added for curing the mixtures, with a small amount of carbon dust to increase the ultrasound scattering property of the phantom. The mixtures were vacuum pumped until no more air bubbles were observed on the surface. Then they were heated at about 60 °C for two hours to increase the speed of curing. The size of the phantom was 100 mm × 80 mm × 20 mm, and the density ranged from 1.05 g/cm^3 to 1.15 g/cm^3 among the phantoms.

Biological tissues were also included for *in vitro* experiments. A large piece of porcine loin sample was obtained from a local slaughterhouse. The porcine loin had a size of about 200 mm × 100 mm × 45 mm, and its weight was 876 g, corresponding to a density of 0.973 g/cm^3.

To reduce the lower boundary reflections, a 35-mm thick silicone phantom, with no carbon dust and a shear modulus of ~100 kPa, was placed under the measured material. The testing sample could also be found in Fig. 3(b). All the measurements were performed at a room temperature of 25 °C.

D. Experimental designs

We compared the coded vibration with the single pulse vibration to test whether the proposed method would enhance the elasticity measurement. In both forms of vibration, an automatic algorithm using the CCF of the displacements at the two scan lines was designed to estimate the shear modulus μ.

To improve the measurement accuracy, three measuring points were selected on each phantom and six points on the porcine muscle due to its larger size. Ten repeated measurements were conducted on each point for repeatability analysis. The measured displacement time shifts at all measuring points were averaged for computing the shear wave velocity. The shear wave was considered to have a planar wavefront,[27] which propagated perpendicular to the scan lines. Thus, at different imaging depths, formula (4) could be used to estimate the shear wave velocity. To evaluate whether the coded vibration outperforms the pulse vibration in different SNR scenarios, the measured results at two different depths were used to compare the two excitations of vibration. For the phantom, the depths were at $z = 10$ mm and 15 mm; for the porcine muscle whose thickness was larger than that of the phantom, the selected depths were $z = 15$ mm and 20 mm.

As a reference, the elasticity of the material was also measured by the classic indentation method,[45] using a material testing machine (Instron ASTM Method Set, Braintree, MA). The diameter of the indenter α was 12 mm. The phantoms were compressed for 2 mm deformation at a rate of 0.5 mm/s and then relaxed at the same deformation rate. During three cycles of compression relaxation, the compression load P (N) and the deformation W (mm) values were recorded. Then the Young's modulus E was calculated by[27,46]

$$E = \frac{(1-\nu^2)}{2\alpha\kappa(\nu, \alpha/h)}\frac{P}{W}, \tag{6}$$

where h is the tissue thickness, ν is the Poisson's ratio and was defined as 0.5 as the silicone phantoms were nearly incompressible.[27] The scaling factor κ (around 1.1 in our experiment) is dependent on ν and the ratio α/h, which provides a theoretical correction for the finite tissue thickness. The shear modulus μ is related to the Young's modulus E by

$$\mu = \frac{E}{2(1+\nu)} = \frac{1}{3}E. \tag{7}$$

For the phantoms used in the experiment, the shear modulus value ranges from 2 to about 400 kPa and for the porcine muscle this value is only on the order of 10 kPa. Each material was also measured on three (or six for the porcine muscle as in the vibro-ultrasound measurements) measuring points, and for each measuring point the measurement was repeated three times. The averaged μ value was then used as a reference for the comparison between the uncoded and coded vibro-ultrasound measurement.

Two additional metrics were used for assessing the measurement. The SNR of the displacement CCF, which is defined as

$$\mathrm{SNR_{CCF}} = 10\log_{10}\left(\frac{\text{signal correlation power}}{\text{noise power}}\right) = 10\log_{10}\left(\frac{\text{CCF peak value}}{\sigma_1^2+\sigma_2^2}\right). \quad (8)$$

Here, the CCF peak value represents the compressed energy of the signal. σ_1 and σ_2 are the standard deviations of the two scan lines in the static period, which stands for the system noise in the two detected displacement waves. For each material, the $\mathrm{SNR_{CCF}}$ was averaged among all measurements at different measuring points and different times. A higher $\mathrm{SNR_{CCF}}$ value indicates a higher concentrated value of the CCF peak, or a lower noise level of the system. When the ultrasound system with fixed imaging parameters was measuring the same position of the same material, the noise level in the displacement wave should be stable and, thus, the metric mainly depends on the signal correlation power. This ratio directly shows whether the coded vibration could increase the energy in the time shift estimation by using the CCF.

The other metric is the normalized standard deviation (NSD) of the measured shear modulus. It was used to evaluate the repeatability of the measurement and defined as the ratio between the standard deviation and the mean value of measured shear modulus among different measuring times

$$\mathrm{NSD} = \frac{\mathrm{std}\,(\mu_i)}{\mathrm{mean}\,(\mu_i)}, \quad (9)$$

where μ_i represents the averaged shear modulus value for the ith measuring time among different positions. The NSD was expressed in percentage. A lower NSD means less difference between different measurements, indicating a higher measuring stability and repeatability.

IV. RESULTS

In this section, the results of the experiments on both phantoms and porcine muscles are presented.

A. Experiments on silicone phantom

A typical displacement waveform from the measurement on phantom is shown in Fig. 4.

The results showed that the coded vibration increased the peak value of the CCF, while the ratio between the mainlobe peak value and the RSLL was maintained to a comparable level. With the same measuring system and the same noise level in the displacement detection, the CCF of the coded wave showed fewer burrs and a higher peak value of the mainlobe than that of the single pulse, as shown in Fig. 4. This indicated that the coding method had a higher robustness against the noise than the single pulse excitation.

The illustration of the CCF peak value and the static segment for calculating σ_1 and σ_2 is also shown in Fig. 4 and the mean $\mathrm{SNR_{CCF}}$ values of each silicone phantom were calculated. Theoretically, the $\mathrm{SNR_{CCF}}$ improvement by the 4-bit Barker code would be up to $10\times\log_{10}(4) = 6\,\mathrm{dB}$, if the pulse were perfectly compressed. Due to the shear wave distortions through its propagation, the displacements at the two scan lines may not be perfectly matched, which limits the $\mathrm{SNR_{CCF}}$ improvement. This can be seen in Fig. 4. The peak value of the CCF in Fig. 4(b) was less than four times of that in Fig. 4(a), mainly due to the deformation of the fourth cycle pulse of line 2 in Fig. 4(b). As previously mentioned, two different measuring depths of $z = 10\,\mathrm{mm}$ and 15 mm were selected to demonstrate the effect of the coded vibration. The averaged $\mathrm{SNR_{CCF}}$ of the displacement detected at each depth is given in Table I. It could be concluded that for each phantom and each imaging depth, the coded vibration scheme ensured a 3.91–5.99 dB higher $\mathrm{SNR_{CCF}}$ than the single pulse, which accords with the theoretical prediction.

Figure 5 gives an illustration of the fitting results between the measured μ values by the vibro-ultrasound system and the indentation method. The results of the two excitations in vibro-ultrasound system were compared. At the depth of 10 mm, a good linear correlation between the vibro-ultrasound result and the indentation result was observed for

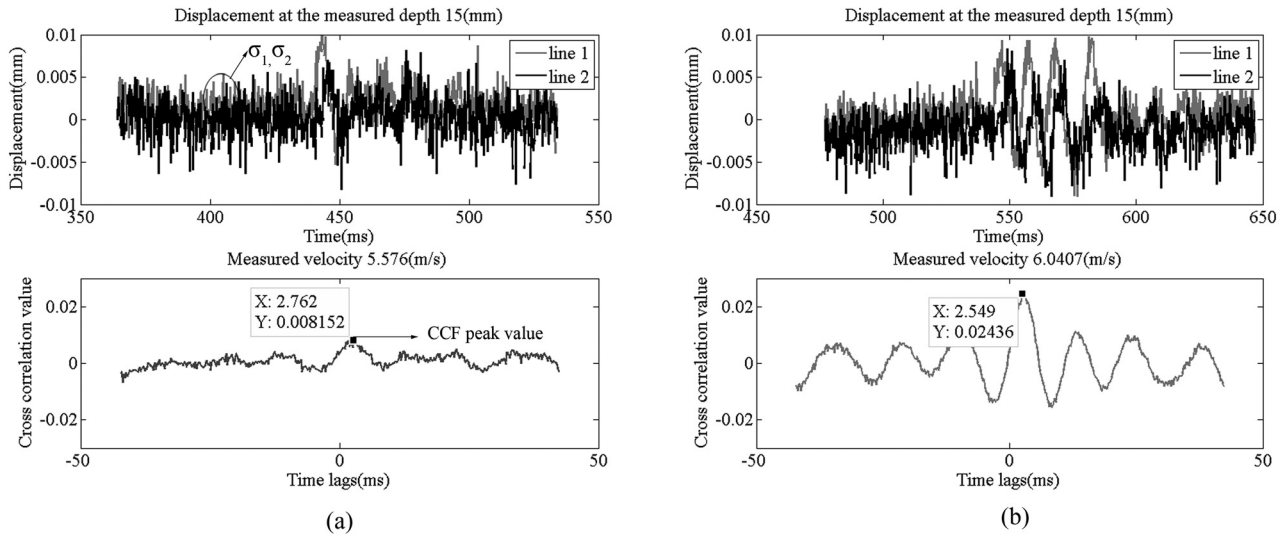

FIG. 4. The displacement waves (top) detected in phantom 2 at $z = 15\,\mathrm{mm}$ and the corresponding CCFs (bottom): (a) the single pulse vibration and (b) the 4-bit Barker coded vibration. σ_1, σ_2, and the CCF peak value are also indicated.

TABLE I. The SNR_{CCF} (dB) of detected displacements at different depths for each phantom.

Phantom number	SNR_{CCF} (dB) ($z = 10$ mm)		SNR_{CCF} (dB) ($z = 15$ mm)	
	Single pulse	Coded pulse	Single pulse	Coded pulse
1	1.96	7.61	−5.71	−1.73
2	4.15	9.31	−4.68	0.87
3	12.49	18.09	−2.65	2.76
4	15.43	21.42	−1.27	5.06
5	10.50	15.56	−3.62	1.92
6	7.03	12.44	−8.83	−4.09
7	4.48	9.67	−6.52	−2.61

TABLE II. Averaged NSD values of measurements at different depths for each phantom.

Phantom number	NSD ($z = 10$ mm)		NSD ($z = 15$ mm)	
	Single pulse	Coded pulse	Single pulse	Coded pulse
1	3.6%	1.5%	6.3%	5.7%
2	6.1%	2.6%	11.9%	6.8%
3	1.7%	0.7%	10.4%	6.3%
4	1.1%	0.5%	9.4%	3.4%
5	3.8%	1.2%	10.5%	8.6%
6	7.3%	2.3%	34.6%	22.8%
7	16.2%	7.7%	40.6%	27.1%

both the single pulse excitation and the Barker coded excitation. However, at a deeper detecting region, where the pulse-echo SNR decreased as previously presented, the measurement accuracy of the vibro-ultrasound system using the single pulse vibration degraded, with the linear correlation between the two measurements decreasing to $y = 0.938x - 1.589$ with an R^2 value of 0.987. Meanwhile, when using the Barker coded vibration, the measurements by the two systems still maintained a good linear correlation of $y = 1.062x - 12.917$ with an R^2 value of 0.993. This demonstrated the advantages of the coded vibration in measuring accuracy.

The NSD values at different depths for each measured phantom are given in Table II. They are also illustrated as error bars in Fig. 5. Due to the relatively higher pulse-echo SNR, the NSD value for each phantom at $z = 10$ mm was lower than that at $z = 15$ mm. By comparison, the coded vibration has a lower NSD value for all phantoms compared with the single pulse vibration. At the depth of 10 mm, the biggest difference between two excitation schemes is about 7.5% (phantom 7). At deeper measuring positions, the NSD value increased in both methods, which indicated an increased difficulty in maintaining the measurement stability. Nevertheless, the coded method showed a much better measuring repeatability. The NSD was about 0.6%–13.5% lower than that of the single pulse method.

B. Experiments on porcine muscle

As previously said, we found that the 100 Hz wave would attenuate rapidly through the 3 cm distance between the vibrator and the edge of the transducer in the porcine muscle study and, thus, the wave frequency was changed to 25 Hz in order to reduce the shear wave attenuation. Other parameters of the experiment were the same as those adopted in the phantom study. Two detecting depths, $z = 15$ mm and 20 mm were selected, as the thickness of the tissue was larger than that of the phantom. Figure 6 illustrates a typical displacement waveform obtained at $z = 20$ mm and the peak values were indicated.

Similar to the phantom study, the coded vibration increased the peak value of the CCF to about four times, which enhanced the robustness against the system noise. The

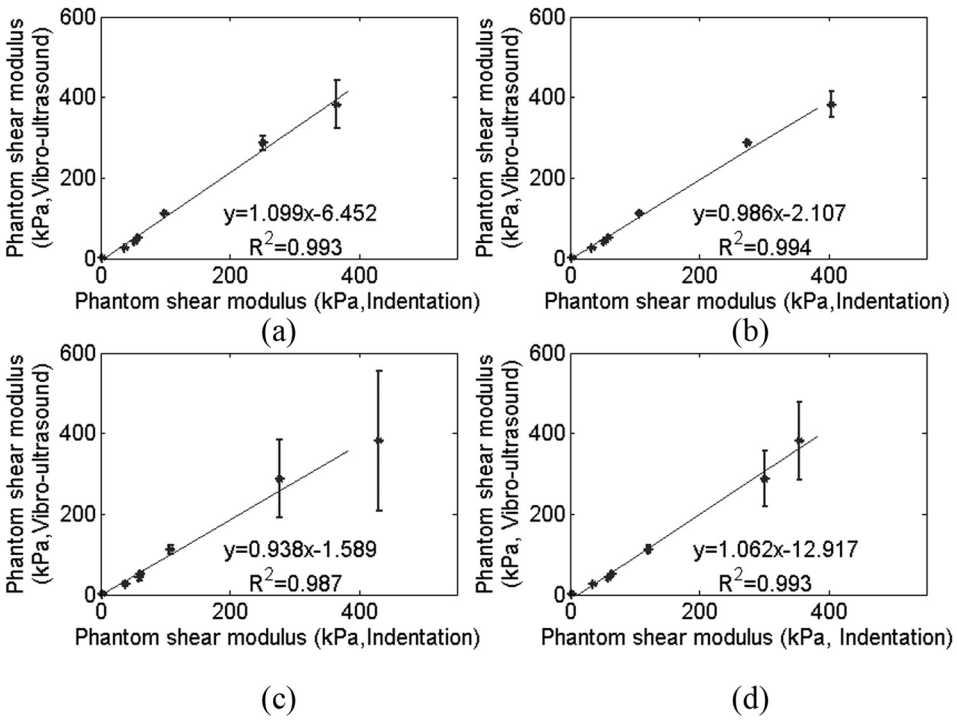

FIG. 5. Phantom results using the vibro-ultrasound system and the indentation method: (a) single pulse vibration at $z = 10$ mm; (b) coded vibration at $z = 10$ mm; (c) single pulse vibration at $z = 15$ mm, (d) coded vibration at $z = 15$ mm. The error bar represents the standard deviation among the ten times of measurements.

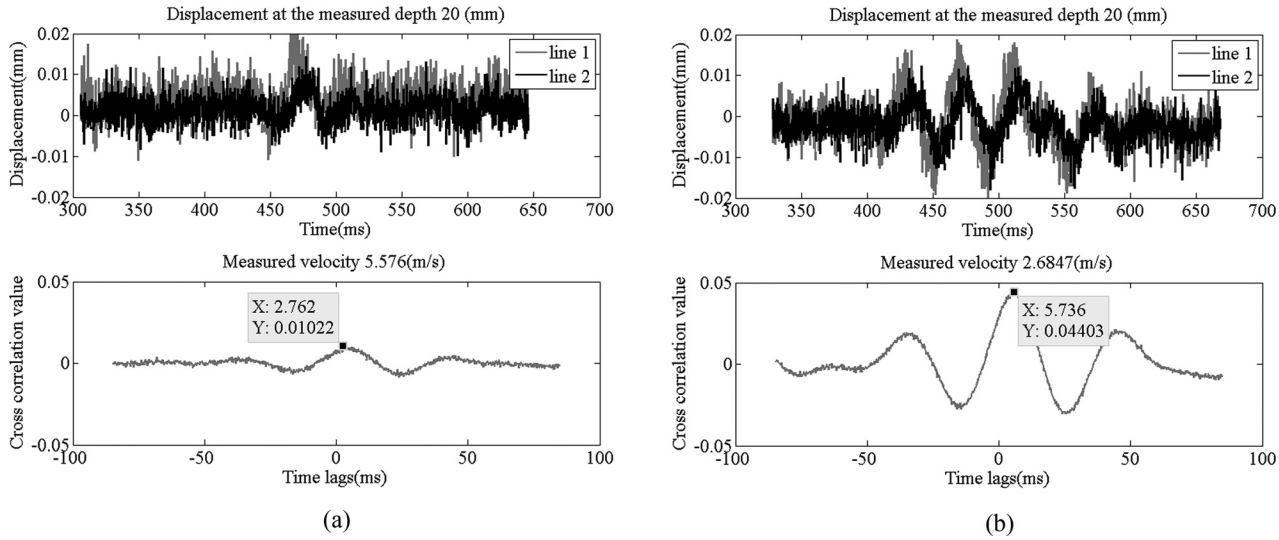

FIG. 6. The displacement waves detected in the porcine muscle (top) at $z = 20$ mm and the corresponding CCFs (bottom): (a) the single pulse vibration and (b) the 4-bit Barker coded vibration.

averaged SNR_{CCF} using the single pulse excitation was 7.63 dB at $z = 15$ mm and -4.51 dB at $z = 20$ mm, while for the 4-bit Barker coded vibration, the SNR_{CCF} value increased to 13.46 dB and 1.11 dB at the two depths, respectively. For the measured shear modulus μ, the single pulse excitation got a value of 5.52 kPa at $z = 15$ mm and 5.89 kPa at $z = 20$ mm, while the corresponding value for the coded excitation was 5.36 kPa and 5.56 kPa, respectively. Meanwhile, the indentation method offered a shear modulus value of 5.34 kPa as a reference. It can be seen that the coded vibration got a closer measurement result, especially when the depth was larger. The NSD value obtained also demonstrated the advantage of the coded vibration. At the depth of 15 mm, the mean NSD value was 4.6% for the single pulse vibration and 3.3% for the 4-bit Barker coded vibration, and at the depth of 20 mm the values increased to 8.2% and 4.0%, respectively. Although increased depth led to the increase of NSD, the coded method still had smaller NSD value than the single pulse excitation, which indicated its higher stability of the measurement.

V. DISCUSSION

In this study, the vibro-ultrasound system provided an averaged single-value estimation of the shear modulus for the tissues between two scan lines. Although the homogeneous model we used was not always accurate for heterogeneous tissue, it could be used to offer an acceptable estimation of the tissue stiffness.[7,16,27] As the measured elasticity is the averaged value within the region between two scan lines, and measurements were conducted at different measuring points and repeated ten times for each point, the influence of the material's heterogeneity was reduced. Due to those averaging implementations, the measured elasticity values at different depths were also considered to be the same, which indicated the overall tissue elasticity. However, a deeper depth usually means a lower pulse-echo SNR due to the ultrasound attenuation, which may degrade the measurement accuracy and repeatability.[28] This could be seen from the lower SNR_{CCF} in Table I and higher NSD in Table II with the depth of 15 mm.

In all cases, the coded vibration for elasticity measurement achieved a higher SNR_{CCF}. The SNR_{CCF} improvement than the single-cycle pulse comes from the higher energy of the 4-cycle time duration. The low RSLL, which was maintained by the coded time sequence, is desired when using the CCF peak value time for time shift estimation. In the phantom study, a deeper detecting depth caused a decreased signal SNR, which weakened the correlation between the results that were obtained using the single pulse vibration and the referenced indentation method. In comparison with single pulse, the coded vibration method preserved a higher linear correlation with the indentation method, resulting from its improvement on the SNR_{CCF}. This improvement also helped to maintain the stability through different times of measurement as the NSD for the coded vibration was 0.6%–13.5% lower than that using the single pulse vibration. For the porcine muscle, the coded vibration method provided a measured elasticity closer to that of the indentation method at a deeper region, and a similar statistical result of the SNR_{CCF} and NSD to that in the phantom study was obtained. In ultrasound B-mode imaging using coded excitation,[33,36,38] the effect of coding in increasing the penetration without resolution decline has been demonstrated. Similarly, the coded shear wave here ideally promised an extended detecting distance with the same excitation amplitude. It is different from the use of the coded excitation for ultrasound signal in elasticity measurement,[41] which still focuses on the enhancement of the ultrasonic imaging system itself. Unlike the coded ultrasound imaging in elastography that benefits the ultrasound imaging penetration, the coding of the shear wave by our method would benefit those tissue elasticity measurements where shear wave penetration may be a main limitation, such as in the liver and kidney.[30] It might also help to enhance the measurement accuracy with low excitation amplitude for safety control, especially for the internal excited shear waves using highly focused ultrasound beam.[3]

These changes are all meaningful in elastography, although further research for demonstration is still required.

The shear wave velocity was estimated by measuring the time shifts. For materials with a higher shear modulus μ, the time shift between the displacement waves at two scan lines should be smaller. Even one time step error of the measured time shift may cause a large difference to the estimation of the shear modulus. This explains why the measured NSD value for phantom 7, which had the highest shear modulus in the experiment, was also the highest among all the phantoms. With the 4.7 kHz frame rate in this study, the time shift may be only several time steps for the hardest phantom. To avoid rapid change in the calculated shear modulus, the displacement wave was resampled with an interpolation factor of 10. Although the ultrasound scanner could only scan two lines with the frame rate, a potential advancement could be achieved by using the plane wave imaging or compounding mode, as in the SSI.[7] Since the plane wave scans the entire imaging region for each beam firing, it could provide the shear modulus estimation at each imaging point instead of the mean value for a block of the material.

In practical application of the coded vibration, the waveform and frequency should be carefully chosen. In this study, the 4-bit Barker code was used. The pulse frequency was set 100 Hz for the silicone phantom and 25 Hz for the tissue. The main factors that need to be considered when designing the excitation waveform are the shear wave dispersion, attenuation, and boundary reflection caused by the finite material size. The dispersion of the shear wave will lead to wave deformation, which is undesirable for the coded wave as the correlation characteristic may be destroyed. Thus, a narrow-band excitation signal is preferred to minimize the effect of dispersion, and that is why the chirp code was not used. On the other hand, since higher frequency components usually attenuate faster than the lower frequency components with the increased propagation distance, a frequency component without rapid decay should be used to ensure the detection of the shear wave. However, a lower frequency means longer time duration of the wave, which will exaggerate the influence by the reflection from different boundaries. Although the boundary reflection was considered in the experiment, it was not totally removed and might be more complicated in clinical settings as human tissues usually contain different anatomic structures. To reduce the effect of the boundary reflection, the pulse time duration should not be too long.

The concept of coded shears waves was validated for external stimulus in elasticity measurement in this study. However, it is still challenging to extend the concept by generating the coded shear waves internally. Considering the advantages of internal vibration techniques using focused ultrasound beams, such as being more patient friendly and easier to control,[30,31] it will be worthwhile to further the investigation using the technique proposed in this study.

VI. CONCLUSIONS

We proposed the concept of using a coded form of vibration in elasticity measurement in this study. The feasibility of the coded vibration concept was evaluated on a vibro-ultrasound platform for measuring elasticity. Experiments were conducted on both phantoms and biological tissues. The results on both materials indicated that compared with single-pulse excitation, the coded vibration increased the SNR_{CCF} of the detected displacement waveforms, while maintaining a low RSLL of the CCF. Using the same time shift estimation algorithm, the increase of SNR_{CCF} benefited the measurement accuracy. In the phantom study, a higher linear correlation ($R^2 = 0.993$) between the phantom result obtained by the vibro-ultrasound system at the depth of 20 mm and that ($R^2 = 0.987$) by the indentation method was observed. In the study of a porcine muscle tissue with a shear modulus of 5.34 kPa, the coded vibration also obtained a shear modulus value that is more accurate than the single-cycle pulse by 0.16 kPa and 0.33 kPa at two different depths Moreover, in all experimental cases, the coded vibration got lower NSD values, which demonstrated an enhancement in repeatability and robustness against the low SNR scenarios. This enhancement should be helpful in achieving a further detecting distance or using a lower excitation amplitude for safety consideration. Although there are still problems on how the coded vibration concept could be more widely applied to elastography, the feasibility of the coded vibration idea has been demonstrated and its potentiality could be further explored.

ACKNOWLEDGMENTS

This work was supported by the National Basic Research Program of China (Grant No. 2015CB755500), the National Natural Science Foundation of China (Grant No. 61271071), and the Joint Supervision Scheme with Mainland China, Taiwan, and Macao University of Hong Kong Polytechnic University (Grant No. G-SB19).

[1]R. M. Lerner, S. R. Huang, and K. J. Parker, "Sonoelasticity images derived from ultrasound signal in mechanically vibrated tissues," Ultrasound Med. Biol. **16**, 231–239 (1990).
[2]J. Ophir, I. Cespedes, H. Ponnekanti, Y. Yazdi, and X. Li, "Elastography: A quantitative method for imaging the elasticity of biological tissues," Ultrason. Imaging **13**, 111–134 (1991).
[3]A. P. Sarvazyan, O. V. Rudenko, S. D. Swanson, J. B. Fowlkes, and S. Y. Emelianov, "Shear wave elasticity imaging: A new ultrasonic technology of medical diagnostics," Ultrasound Med. Biol. **24**, 1419–1435 (1998).
[4]S. Catheline, F. Wu, and M. Fink, "A solution to diffraction biases in sonoelasticity: The acoustic impulse technique," J. Acoust. Soc. Am. **105**, 2941–2950 (1999).
[5]L. Sandrin, M. Tanter, S. Catheline, and M. Fink, "Shear modulus imaging with 2-D transient elastography," IEEE Trans. Ultrason. Ferroelectr. Freq. Control **49**, 426–435 (2002).
[6]M. Tanter, J. Bercoff, L. Sandrin, and M. Fink, "Ultrafast compound imaging for 2-D motion vector estimation: Application to transient elastography," IEEE Trans. Ultrason. Ferroelectr. Freq. Control **49**, 1363–1374 (2002).
[7]J. Bercoff, M. Tanter, and M. Fink, "Supersonic shear imaging: A new technique for soft tissue elasticity mapping," IEEE Trans. Ultrason. Ferroelectr. Freq. Control **51**, 396–409 (2004).
[8]S. Chen, M. W. Urban, C. Pislaru, R. Kinnick, Y. Zheng, A. Yao, and J. F. Greenleaf, "Shearwave dispersion ultrasound vibrometry (SDUV) for measuring tissue elasticity and viscosity," IEEE Trans. Ultrason. Ferroelectr. Freq. Control **56**, 55–62 (2009).
[9]T. Deffieux, G. Montaldo, M. Tanter, and M. Fink, "Shear wave spectroscopy for *in vivo* quantification of human soft tissues visco-elasticity," IEEE Trans. Med. Imaging **28**, 313–322 (2009).

[10]J. B. Fowlkes, S. Y. Emelianov, J. G. Pipe, A. R. Skovoroda, P. L. Carson, R. S. Adler, and A. P. Sarvazyan, "Magnetic-resonance imaging techniques for detection of elasticity variation," Med. Phys. **22**, 1771–1778 (1995).
[11]A. Manduca, T. E. Oliphant, M. A. Dresner, J. L. Mahowald, S. A. Kruse, E. Amromin, J. P. Felmlee, J. F. Greenleaf, and R. L. Ehman, "Magnetic resonance elastography: Non-invasive mapping of tissue elasticity," Med. Image Anal. **5**, 237–254 (2001).
[12]F. Ciampa and M. Meo, "Nonlinear elastic imaging using reciprocal time reversal and third order symmetry analysis," J. Acoust. Soc. Am. **131**, 4316–4323 (2012).
[13]E. Ehman and A. Manduca, "Magnetic resonance elastography," J. Acoust. Soc. Am. **117**, 2587 (2005).
[14]I. Cespedes, J. Ophir, H. Ponnekanti, and N. Maklad, "Elastography: Elasticity imaging using ultrasound with application to muscle and breast *in-vivo*," Ultrason. Imaging **15**, 73–88 (1993).
[15]M. Odonnell, A. R. Skovoroda, B. M. Shapo, and S. Y. Emelianov, "Internal displacement and strain imaging using ultrasonic speckle tracking," IEEE Trans. Ultrason. Ferroelectr. Freq. Control **41**, 314–325 (1994).
[16]S. Catheline, J. L. Thomas, F. Wu, and M. A. Fink, "Diffraction field of a low frequency vibrator in soft tissues using transient elastography," IEEE Trans. Ultrason. Ferroelectr. Freq. Control **46**, 1013–1019 (1999).
[17]L. Sandrin, S. Catheline, and M. Fink, "Transient elastography in biological tissues," J. Acoust. Soc. Am. **105**, 1014–1015 (1995).
[18]S. F. Levinson, M. Shinagawa, and T. Sato, "Sonoelastic determination of human skeletal-muscle elasticity," J. Biomech. **28**, 1145–1154 (1995).
[19]K. R. Nightingale, M. L. Palmeri, R. W. Nightingale, and G. E. Trahey, "On the feasibility of remote palpation using acoustic radiation force," J. Acoust. Soc. Am. **110**, 625–634 (2001).
[20]K. Nightingale, M. S. Soo, R. Nightingale, and G. Trahey, "Acoustic radiation force impulse imaging: *In vivo* demonstration of clinical feasibility," Ultrasound Med. Biol. **28**, 227–235 (2002).
[21]M. Tanker, M. Pernot, J. L. Gennisson, and M. Fink, "A review of the medical applications of shear wave elastography," J. Acoust. Soc. Am. **134**, 4009 (2013).
[22]S. G. Chen, M. Fatemi, and J. F. Greenleaf, "Quantifying elasticity and viscosity from measurement of shear wave speed dispersion," J. Acoust. Soc. Am. **115**, 2781–2785 (2004).
[23]C. Amador, M. W. Urban, S. Chen, and J. F. Greenleaf, "Shearwave dispersion ultrasound vibrometry (SDUV) on swine kidney," IEEE Trans. Ultrason. Ferroelectr. Freq. Control **58**, 2608–2619 (2011).
[24]Y. Zhu, X. Zhang, Y. Zheng, X. Chen, Y. Shen, H. Lin, Y. Guo, T. Wang, and S. Chen, "Quantitative analysis of liver fibrosis in rats with shearwave dispersion ultrasound vibrometry: Comparison with dynamic mechanical analysis," Med. Eng. Phys. **36**, 1401–1407 (2014).
[25]L. Sandrin, B. Fourquet, J. M. Hasquenoph, S. Yon, C. Fournier, F. Mal, C. Christidis, M. Ziol, B. Poulet, F. Kazemi, M. Beaugrand, and R. Palau, "Transient elastography: A new noninvasive method for assessment of hepatic fibrosis," Ultrasound Med. Biol. **29**, 1705–1713 (2003).
[26]S. Dos Santos, B. Choi, A. Sutin, and A. Sarvazyan, "Nonlinear imaging based on time reversal acoustic focusing," in *Proceedings of the 8th French Congress of Acoustics* (2006), pp. 359–362.
[27]C.-Z. Wang, T.-J. Li, and Y.-P. Zheng, "Shear modulus estimation on vastus intermedius of elderly and young females over the entire range of isometric contraction," PLoS One **9**, e101769 (2014).
[28]M. W. Urban, S. Chen, and J. F. Greenleaf, "Error in estimates of tissue material properties from shear wave dispersion ultrasound vibrometry," IEEE Trans. Ultrason. Ferroelectr. Freq. Control **56**, 748–758 (2009).
[29]H. Zhang, S. Wu, D. Ta, K. Xu, and W. Wang, "Coded excitation of ultrasonic guided waves in long bone fracture assessment," Ultrasonics **54**, 1203–1209 (2014).
[30]M. L. Palmeri and K. R. Nightingale, "Acoustic radiation force-based elasticity imaging methods," Interface Focus **1**, 553–564 (2011).
[31]J. R. Doherty, G. E. Trahey, K. R. Nightingale, and M. L. Palmeri, "Acoustic radiation force elasticity imaging in diagnostic ultrasound," IEEE Trans. Ultrason. Ferroelectr. Freq. Control **60**, 685–701 (2013).
[32]M. Muller, J.-L. Gennisson, T. Deffieux, M. Tanter, and M. Fink, "Quantitative viscoelasticity mapping of human liver using supersonic shear imaging: Preliminary *in vivo* feasability study," Ultrasound Med. Biol. **35**, 219–229 (2009).
[33]M. Odonnell, "Coded excitation system for improving the penetration of real-time phased-array imaging-systems," IEEE Trans. Ultrason. Ferroelectr. Freq. Control **39**, 341–351 (1992).
[34]R. Kazys, L. Svilainis, and L. Mazeika, "Application of orthogonal ultrasonic signals and binaural processing for imaging of the environment," Ultrasonics **38**, 171–175 (2000).
[35]T. X. Misaridis, K. Gammelmark, C. H. Jorgensen, N. Lindberg, A. H. Thomsen, M. H. Pedersen, and J. A. Jensen, "Potential of coded excitation in medical ultrasound imaging," Ultrasonics **38**, 183–189 (2000).
[36]R. Y. Chiao and X. Hao, "Coded excitation for diagnostic ultrasound: A system developer's perspective," in *2003 IEEE Ultrasonics Symposium Proceedings*, edited by D. E. Yuhas and S. C. Schneider (IEEE, New York, 2003), Vols. 1 and 2, pp. 437–448.
[37]M. P. Mienkina, C.-S. Friedrich, N. C. Gerhardt, M. F. Beckmann, M. F. Schiffner, M. R. Hofmann, and G. Schmitz, "Multispectral photoacoustic coded excitation imaging using unipolar orthogonal Golay codes," Opt. Express **18**, 9076–9087 (2010).
[38]J. Song, S. Kim, H.-Y. Sohn, T.-K. Song, and Y. M. Yoo, "Coded excitation for ultrasound tissue harmonic imaging," Ultrasonics **50**, 613–619 (2010).
[39]S. Dos Santos and Z. Prevorovsky, "Imaging of human tooth using ultrasound based chirp-coded nonlinear time reversal acoustics," Ultrasonics **51**, 667–674 (2011).
[40]G. Armanavičius and R. Kažys, "Digital signal processing in ultrasonic multi-channel measurements," Ultragarsas "Ultrasound" **43**, 21–27 (2014).
[41]P. Song, M. W. Urban, A. Manduca, J. F. Greenleaf, and S. Chen, "Coded excitation plane wave imaging for shear wave motion detection," IEEE Trans. Ultrason. Ferroelectr. Freq. Control **62**, 1356–1372 (2015).
[42]F. Genna, L. Annovazzi, C. Bonesi, P. Fogazzi, and C. Paganelli, "On the experimental determination of some mechanical properties of porcine periodontal ligament," Meccanica **43**, 55–73 (2008).
[43]S. Dos Santos, D. Remache, M. Gratton, and M. Caliez, "Skin hysteretic behavior using acousto-mechanical imaging and nonlinear time reversal signal processing," in *Proceedings of the 22nd International Congress on Sound and Vibration, Major Challenges in Acoustics, Noise and Vibration Research* (2015).
[44]Y.-C. Fung, *Biomechanics: Mechanical Properties of Living Tissues* (Springer Science and Business Media, New York, 2013).
[45]Y. P. Zheng, A. F. T. Mak, and B. Lue, "Objective assessment of limb tissue elasticity: Development of a manual indentation procedure," J. Rehabil. Res. Dev. **36**, 71–85 (1999).
[46]W. C. Hayes, G. Herrmann, L. F. Mockros, and L. M. Keer, "Mathematical-analysis for indentation tests of articular-cartilage," J. Biomech. **5**, 541–551 (1972).